



Quantum-mechanical study of the electronic properties of $U_xPu_yO_z$ compounds formed during the recovery of spent nuclear fuel

ALEXANDER Y. GALASHEV*, ALEXEY S. VOROB'EV and YURI P. ZAIKOV

Institute of High Temperature Electrochemistry, Ural Branch, Russian Academy of Sciences,
Yekaterinburg, Russia

(Received 13 February, revised 22 March, accepted 8 July 2023)

Abstract: A promising way to recover spent nuclear fuel (SNF) is the method of extracting transuranium compounds from molten salt, which makes it possible to obtain a partial separation between transuranium compounds and lanthanides. This work is devoted to the quantum mechanical study of changes in the structure, energy and electronic properties of the main SNF component, uranium dioxide, upon the removal of oxygen from the system. The influence of the considered properties on the substitution of uranium by plutonium is also studied at a ratio, of the number of plutonium atoms to uranium atoms, of 1:7 and 1:3. The removal of oxygen leads to a narrowing of the band gap up to the transition to a conductive state at a ratio of uranium to oxygen of 2:3. The band gap narrows and metallization sets in even when uranium is replaced by plutonium. A two-stage UO_2 metallization scheme based on lithium reduction and direct (electronic) reduction is proposed.

Keywords: geometric and band structures; oxides; plutonium; SNF recovery; spectrum of electronic states; uranium.

INTRODUCTION

The uranium–oxygen system seems to be an extremely complex system, the literature data on which are very contradictory.¹ There are reports in the literature about 14 types of oxides ranging from UO to UO_3 . A number of uranium oxides have several crystalline modifications. Data on the physicochemical properties of these systems are of great importance, since stable compound UO_2 is a reactor fuel. The basis of ceramic nuclear fuel, *i.e.*, UO_2 , has high corrosion, radiation and thermal stability. The high density of UO_2 provides a high concentration of fissile material. The production of electricity using a nuclear reactor does not emit greenhouse gases. Nuclear reactors have a very high energy density. Thus,

* Corresponding author. E-mail: alexander-galashev@yandex.ru
<https://doi.org/10.2298/JSC230213038G>

when one fuel pellet weighing 10 g is burned in a reactor, energy released is equivalent to the energy obtained by burning ~1300 kg of coal, ~1 m³ of oil or ~150 m³ of natural gas.² However, the low thermal conductivity of UO₂ leads to high temperature gradients, which limits the size of the products. In addition, the thermal conductivity of the fuel during its lifetime in the reactor is greatly reduced (up to 70 %).³ Uranium oxides seem to be the most stable compounds of this element, which makes them suitable for storing uranium. Uranium oxides can act as intermediates in the production of other uranium compounds, such as fluorides.

The similar atomic weights and the largely similar atomic structure of uranium and plutonium create prerequisites for considering their effect on the near atomic environment to be practically identical. As a result, the same interaction potentials are used in molecular dynamics modeling of U and Pu.⁴

Electrical conductivity is the physical property that is determined by the electronic structure, has a feedback with it and affects the formation of a new phase. A change in electrical conductivity caused by any process can accelerate or slow down the development of this process. The reduction of uranium dioxide (UO₂) to uranium metal is reduced with the removal of oxygen from the system. The electrolytic reduction method involves the removal of oxygen from UO₂ by displacing uranium from this compound with lithium. The newly formed Li₂O compound enters the salt melt, where it decomposes into Li⁺ and O²⁻. During the electrolytic reduction of spent nuclear fuel (SNF), as a rule, U and Pu simultaneously deposited on the cathode. The U³⁺ reduction potential to metallic U⁰ is only 0.34 eV higher than that of Pu³⁺.⁵ The subsequent separation of the alloy, consisting of U and Pu, requires additional operations.⁶ In the field of pyroprocessing of SNF, liquid cadmium is applied to recover transuranics from molten salt and provide some degree of separations between transuranics and lanthanides. Analytical analysis using experimental data shows that in SNF recovery using a liquid Cd cathode, when both U and Pu are dissolved in cadmium, the highest Pu:U ratio is 8:1, and the lowest Pu:U ratio is 1:4.⁷ Expectedly higher is the proportion of plutonium in binary (U–Pu) metallic fuel intended for fast reactors. In such a non-irradiated fuel, the Pu:U ratio approximately corresponds to a ratio of 1:3, while the proportion of Pu in the irradiated fuel increases significantly.⁸ Hubbard corrected density functional theory (DFT+U), than study of the electronic and thermal properties of stoichiometric and hypostoichiometric phases of uranium dioxide was carried out by Kaloni *et al.*⁹ It was shown that the removal of oxygen can affect the electronic and thermal transport properties of UO₂. In addition, such properties of hypostoichiometric UO₂ as electronic properties, electronic thermal conductivity, phonon dispersion and lattice thermal conductivity were calculated. A change in the electronic properties during SNF recovery can affect the rate of recovery and the completeness of this process.

Therefore, establishing the degree of electrical conductivity of the intermediate phases is important for controlling the mode of the SNF recovery process.

The purpose of this work is to study changes in the structural, energy and electronic properties of uranium dioxide systems, as well as uranium oxides containing plutonium, when the Pu:U ratio is 1:7 and 1:3, when oxygen atoms are removed from the system.

EXPERIMENTAL

These calculations were performed using the Siesta software package.¹⁰ In the work, a study was made of the reduction of uranium dioxide, as well as the effect of the presence of plutonium on the structures energy and electronic properties of uranium oxides. Uranium dioxide was modeled by combining a 2×2×2 uranium FCC supercell (8 uranium atoms) and two cubic oxygen lattices (16 oxygen atoms). In what follows, we will represent the U₈O₁₆ system as UO₂, and the U₈O₁₂ system as U₂O₃. The structure of uranium dioxide after geometric optimization is shown in Fig. 1a. To simulate the reduction of uranium dioxide, two and four oxygen atoms were removed from the supercell; systems containing 14 and 12 oxygen atoms were considered. Fig. 1b shows the structure of U₂O₃, containing 8 uranium atoms and 12 oxygen atoms after geometric optimization. The introduction of plutonium is represented by the replacement of one or two U atoms in 2×2×2 uranium FCC supercell by Pu atoms. Thus, we considered systems with the Pu/U ratio in the uranium dioxide structure 1:7 (1 plutonium atom to 7 uranium atoms) and 1:3 (1 plutonium atom to 3 uranium atoms). The simulation was carried out using the LDA+U approximation,¹¹ the values of the parameters U_{eff} and J_{eff} for both uranium and plutonium atoms were taken to be 4.5 and 0.5 eV, respectively. In all systems considered by us, geometric optimization was carried out using the local density approximation in the CA form.¹² The dynamic relaxation of atoms continued until the change in the total energy of the system became less than 0.001 eV. In the *ab initio* calculations, the Born–Karman periodic boundary conditions were used. The density of the three-dimensional grid used to calculate the electron density was set using a cutoff energy of 550 Ry. The partial density electronic of states (PDOS) and band structures are often used to characterize the electronic properties of materials. The band structure was calculated in the L-Γ-X-U-K-Γ direction. The Brillouin zone was set by the Monkhorst-Pack method¹³ using 5×5×5 k -points.

The binding energies of a uranium or plutonium atom with the rest of the compound (*i.e.*, compound without uranium or plutonium atom) were calculated according to the expression:

$$E_{\text{bond}}^{\text{1U/1Pu}} = -\frac{E_{\text{Tot}} - E_1 - E_{1A}}{N} \quad (1)$$

where E_{Tot} is the total energy of the system, E_1 is the total energy calculated for the system in the absence of a uranium or plutonium atom, E_{1A} is the energy calculated for a single uranium or plutonium atom, and N is the number of atoms in the system.

The energy of bonds between atoms in a compound:

$$E_{\text{bond}} = -\frac{E_{\text{Tot}} - N_O E_{1O} - N_{\text{Pu}} E_{1\text{Pu}} - N_U E_{1U}}{N} \quad (2)$$

where E_{1O} , $E_{1\text{Pu}}$, E_{1U} are the energies calculated for single oxygen, plutonium and uranium atoms, respectively, and N_O , N_{Pu} , N_U are the number of oxygen, plutonium and uranium atoms in the system, respectively.

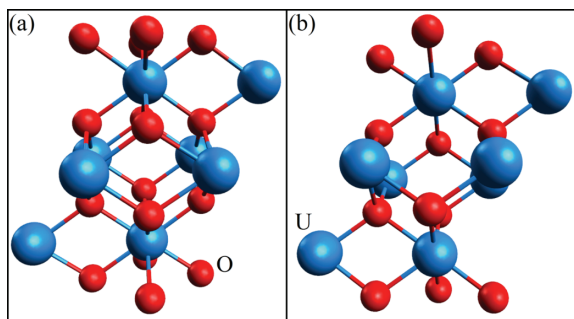


Fig. 1. Geometric structure of: a) UO_2 and b) U_2O_3 after geometric optimization.

RESULTS AND DISCUSSION

Table I represents the following system characteristics: the average binding energy between atoms in the entire system (E_b); the binding energy between the uranium atom and the rest of the system (E_b^{U}); binding energy between a plutonium atom and the rest of the system (E_b^{Pu}); bond lengths between atoms of uranium and oxygen ($L_{(\text{U}-\text{O})}$) and that of plutonium and oxygen ($L_{(\text{Pu}-\text{O})}$). It can be seen that the replacement of uranium atoms in the UO_2 compound by plutonium atoms up to get ratios of plutonium to uranium ($N_{\text{Pu}}/N_{\text{U}}$) of 1:7 and 1:3 leads to a decrease in the binding energy E_b by 1.9 and 4.8 %, respectively. The removal of oxygen in the absence of a plutonium in the system leads to a gradual decrease in the binding energy E_b to 2.2 %. However, E_b behaves differently in the presence of plutonium. An increase in the number of oxygen vacancies similarly have affect on the values of E_b in systems with the ratio ($N_{\text{Pu}}/N_{\text{U}}$) of 1:7 and 1:3. In the hypothetical compound $\text{U}_7\text{PuO}_{14}$ and $\text{U}_6\text{Pu}_2\text{O}_{14}$, the energy E_b increases by 0.3 and 2.5 %, respectively. However, after further withdrawal of oxygen, *i.e.*, in the $\text{U}_7\text{PuO}_{12}$ and $\text{U}_6\text{Pu}_2\text{O}_{12}$ compounds, the energy E_b decreases. The calculation of the energies E_b^{U} and E_b^{Pu} was carried out for 4 different uranium atoms; the table shows the average values of the calculated bond energies. In all considered cases, the energy E_b^{U} decreases on removal of oxygen from the system. The largest drop in energy E_b^{U} equal to 25.5 % is observed when 4 oxygen atoms are removed from the $\text{U}_7\text{PuO}_{16}$ compound. At the same time, the bond energy E_b^{Pu} increases when oxygen is withdrawn from plutonium containing systems. Thus, when 4 oxygen atoms were removed from the $\text{U}_7\text{PuO}_{16}$ and $\text{U}_6\text{Pu}_2\text{O}_{16}$ systems, the energy of E_b^{Pu} increased by 34.0 and 13.3 %, respectively.

The lengths of the $\text{U}-\text{U}$ and $\text{Pu}-\text{U}$ bonds in all the considered compounds are practically unchanged and are approximately equal to 3.81 and 3.79 Å, respectively. This agrees with the data of a small displacement of uranium atoms in hypostoichiometric UO_{2-x} compounds.⁹ The $\text{U}-\text{O}$ lengths upon replacement of one or two U atoms by Pu atoms in U_8O_y compounds decrease from 1.5 to 2.2 %

depending on the composition of the hypothetical compound. In all cases a slight decrease, from 0.1 to 1 % in the lengths, of the U–O bonds was found when 4 oxygen atoms were removed from the systems (UO₂, U₇PuO₁₆ and U₆Pu₂O₁₆). While the Pu–O bond lengths during the transition from the U₇PuO₁₆ and U₆Pu₂O₁₆ to U₇PuO₁₂ and U₆Pu₂O₁₂ hypothetical compounds increase by 2.1 and 3.3 %, respectively.

TABLE I. Characteristics of systems U_{8-x}Pu_xO_y (x and y is the number of plutonium and oxygen atoms in the system, respectively); E_b – bond energy of atoms in the system, E_b^{lU} , E_b^{lPu} – energy of bonds between 1 atom of uranium/plutonium with the rest of the system, $L_{(U-O)}$, $L_{(Pu-O)}$ – average bond lengths between uranium/plutonium and oxygen atoms

N_{Pu}	N_O	E_b / eV	E_b^{lU} / eV	E_b^{lPu} / eV	$L_{(U-O)}$ / Å	$L_{(Pu-O)}$ / Å
0	16	11.527	2.159	–	2.321	–
	14	11.406	2.113	–	2.314	–
	12	11.273	2.106	–	2.313	–
1	16	11.306	3.015	2.499	2.279	2.388
	14	11.345	2.515	3.240	2.279	2.426
	12	11.126	2.244	3.349	2.276	2.439
2	16	10.971	2.603	2.081	2.286	2.329
	14	11.248	2.492	2.280	2.278	2.369
	12	11.047	2.429	2.358	2.263	2.406

Fig. 2 shows the band structures of the considered systems, and Table II presents the electronic properties of the systems containing plutonium. The band gap obtained for uranium dioxide is 2.23 eV, which is slightly larger than the value of 2.19 eV obtained earlier.¹⁴ The removal of two oxygen atoms from the UO₂ system leads to a narrowing of the band gap to 0.99 eV. If we continue to remove oxygen from the system in the same amount (*i.e.*, remove 2 more O atoms), then the system becomes conductive. The narrowing of the band gap and the transition to a conducting phase in hypostoichiometric uranium compounds are consistent with the data previously obtained.⁹ Substitution of uranium by plutonium at ratios of $N_{Pu}/N_U = 1:7$ and $1:3$ leads to metallization of the U₇PuO₁₂, U₆Pu₂O₁₆, U₆Pu₂O₁₄ and U₆Pu₂O₁₂ systems, while the U₇PuO₁₆ and U₇PuO₁₄ systems have semiconductor properties.

Fig. 3 shows the partial density of the electronic states for the UO₂, U₂O₃, U₇PuO₁₂ and U₆Pu₂O₁₆ systems. It can be seen that the conductive properties in hypothetical compound U₂O₃ appear due to the interaction of the d and f orbitals of uranium with the p orbitals of oxygen. The Fermi level turns out to be slightly shifted into the conduction band of U₂O₃, and the width of the a band gap is ~0.1 eV. At the same time, in the PDOS spectra of U₇PuO₁₂ and U₆Pu₂O₁₆, the valence band continuously passes into the conduction band. Moreover, conductivity appears in these compounds due to the interaction of 6d uranium orbitals with 5f plutonium orbitals and 5f uranium and plutonium orbitals with 2p oxygen orb-

itals, respectively. In the PDOS of the $\text{U}_7\text{PuO}_{12}$ compound, a high bimodal peak related to the 5f electrons of uranium is in the valence band, while in the PDOS of the $\text{U}_6\text{Pu}_2\text{O}_{16}$ compound, a similarly shaped peak also related to the 5f electrons of uranium appears in the conduction band. For the three connections (UO_2 , U_2O_3 , $\text{U}_6\text{Pu}_2\text{O}_{16}$) shown in the figure in the PDOS spectrum, there are adjacent bands not wide enough to span the full range of electron energy levels. In the PDOS spectrum of $\text{U}_7\text{PuO}_{16}$, there are no such adjacent allowed bands. In other words, in this case the part of the spectrum that belongs to the valence band is continuous.

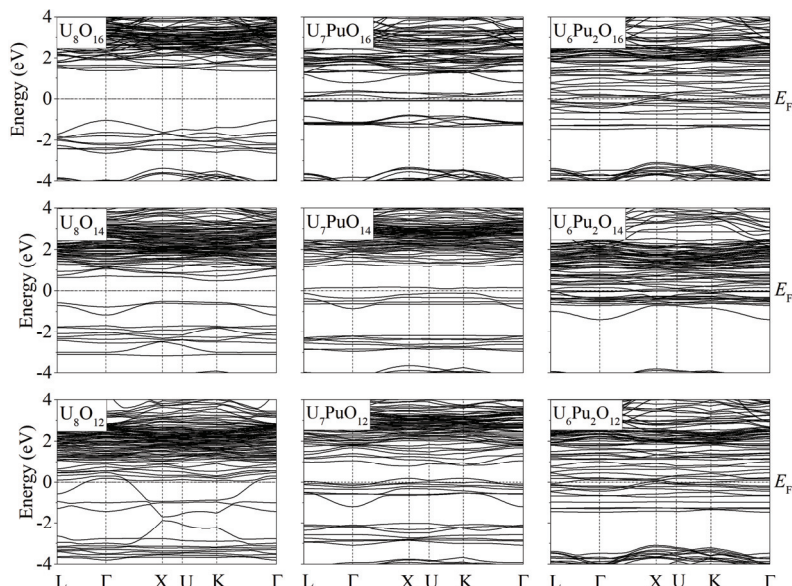


Fig. 2. Band structures obtained for compounds U_8O_{16} , U_8O_{14} , U_8O_{12} , $\text{U}_7\text{PuO}_{16}$, $\text{U}_7\text{PuO}_{14}$, $\text{U}_7\text{PuO}_{12}$, $\text{U}_6\text{Pu}_2\text{O}_{16}$, $\text{U}_6\text{Pu}_2\text{O}_{14}$ and $\text{U}_6\text{Pu}_2\text{O}_{12}$.

TABLE II. Conductivity characteristics of uranium oxide systems containing plutonium

Compound	Electronic properties	Band gap, eV	Compound	Electronic properties	Band gap, eV
$\text{U}_7\text{PuO}_{16}$	Semiconductor	0.07	$\text{U}_6\text{Pu}_2\text{O}_{16}$	Metal	—
$\text{U}_7\text{PuO}_{14}$	Semiconductor	0.21	$\text{U}_6\text{Pu}_2\text{O}_{14}$	Metal	—
$\text{U}_7\text{PuO}_{12}$	Metal	—	$\text{U}_6\text{Pu}_2\text{O}_{12}$	Metal	—

The presence of many different phases of non-stoichiometric actinide oxides (AO_x), complex structures and their tendency to form solid solutions make it extremely difficult to understand not only the structure, but also chemical composition. Nevertheless, the DFT+U calculations reflect the correct trend of the band gap depending on the oxidation state of the actinides.¹⁵

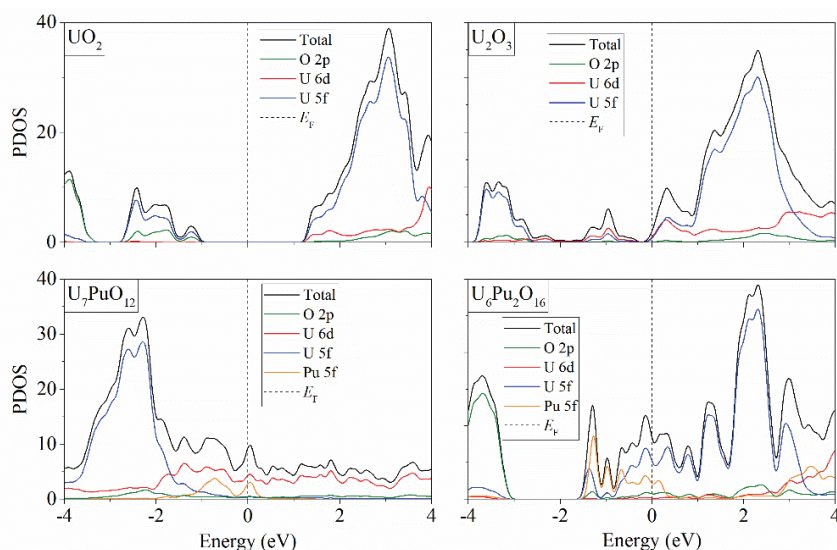


Fig. 3. Partial density of electronic states obtained for compounds UO_2 , U_2O_3 , U_7PuO_{12} and $U_6Pu_2O_{16}$.

The reduction of UO_2 to uranium metal in the molten salt of LiCl with the addition of Li_2O takes place in close contact with the cathode and is an electrochemical process. We now represent the process of reduction of UO_2 by chemical reactions. The presence of the electrical conductivity in the U_2O_3 phase allows us to understand more deeply the process of electrochemical pyrolysis that we consider. A small ($\sim 3\%$) initial addition of Li_2O to the LiCl electrolyte leads to an imbalance between Li^+ and Cl^- in the salt melt and the creation of the necessary double charged layer near the surface of the UO_2 pellet after creating a certain electrical voltage (3.0–3.3 V) between the electrodes. In general, the decay of Li_2O can be represented as:



O^{2-} formed after the decay of Li_2O can quickly reach the anode, because O^{2-} are 2.2 times lighter than Cl^- . In addition, their electric charge is 2 times greater than that of Cl^- . Each O^{2-} gives out 2 electrons at the anode. The formed O atoms combine into O_2 molecules which form bubbles that rise and remove oxygen from the system.

To simplify, let us consider the SNF recovery process using pure UO_2 as an example. The first stage of the process mainly involves the external part (that is directly in contact with the electrolyte) of the UO_2 pellet. After the formation of a double electric layer between the surface of a highly polarized semiconductor (UO_2) and the near-surface part of an electrolyte (LiCl) strongly enriched with

Li^+ , a strong local electric field arises and “pulls” oxygen ions from the surface of the semiconductor:



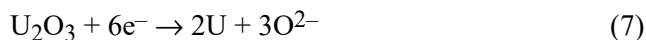
In the near-surface region of the electrolyte, O^{2-} combines with two Li^+ to form an electrically neutral molecule Li_2O :



The second stage of recovery begins with the electronically conductive metallized $(\text{U}_2\text{O}_3)^{2+}$ and with an excess of positive charge takes the missing electrons thus becomes electrically neutral, but the conducting substance:



The continuation of the second stage of reduction is associated exclusively with the electrical conductivity of the intermediate U_2O_3 phase. The electrically conductive surface layer continues to receive electrons and U_2O_3 is reduced to the metallic uranium:



The mechanism for the reduction of UO_2 to metallic U presented here is supported by experimental facts, among which are the movement of the metallization front from the surface to the center of the pellet and the absence of lithium inside the pellet with a 98 % reduced metal U.⁵⁻⁸ In addition, the reduction process actively occurs in a high-quality sintered UO_2 powder granule, but quickly fades if the spent fuel used for recovery is taken in the form of a conventional powder.

A significant increase in the electronic contribution for certain compositions of oxide nuclear fuel contributes to an increase in thermal conductivity.⁹ We have shown that this conclusion is also valid in the presence of Pu in the fuel. Thus, the use of hypostoichiometric phases seems to be favorable for obtaining a fuel that is resistant to accidents.

CONCLUSION

In this work, based on quantum mechanical calculations, the partial reduction of uranium and uranium-plutonium oxides is studied. The change in the structure, energy, and electronic properties of these oxides was studied when uranium atoms were replaced by plutonium atoms up to the ratio of the number of atoms in the system $N_{\text{Pu}}/N_{\text{U}} = 1:7$ and $1:3$. A decrease in the total bond energy in the UO_2 compound is shown when uranium is replaced by plutonium in the ratios $N_{\text{Pu}}/N_{\text{U}} = 1:7$ and $1:3$. An increase in the bond energy between plutonium and the rest of the compound was revealed upon the removal of oxygen from the $\text{U}_7\text{PuO}_{16}$ and $\text{U}_6\text{Pu}_2\text{O}_{16}$ systems. It is shown that the band gap narrows up to complete metallization of the compound when oxygen is removed from the UO_2

compound to the ratio $N_U/N_O = 2:3$. A transition to the conducting state of the UO_2 compound was revealed when uranium was replaced by plutonium in the ratios $N_{Pu}/N_U = 1:3$. A two-stage process of uranium metallization during its reduction in $LiCl-Li_2O$ melt is proposed. We hope that this study will improve understanding of the SNF electrolytic reduction process and serve as a stimulus for its optimization.

Acknowledgements. The calculations were performed on a hybrid cluster-type computer “URAN” at the Institute of Mathematics and Mechanics, Ural Branch of the Russian Academy of Sciences with a peak performance of 216 Tflop/s and 1864 CPUs. The work is executed within the framework of the multipurpose program “Development of equipment, technologies and scientific research in the field of the use of atomic energy in the Russian Federation for the period up to 2024”.

ИЗВОД

КВАНТНО-МЕХАНИЧКА СТУДИЈА ЕЛЕКТРОНСКИХ ОСОБИНА $U_xPu_yO_z$ ЈЕДИЊЕЊА ФОРМИРАНИХ ТОКОМ ОБНАВЉАЊА ИСТРОШЕНОГ НУКЛЕАРНОГ ГОРИВА

ALEXANDER Y. GALASHEV, ALEXEY S. VOROB'EV и YURI P. ZAIKOV

Institute of High Temperature Electrochemistry, Ural Branch, Russian Academy of Sciences, Yekaterinburg, Russia

Објављујући начин за обнављање истрошеног нуклеарног горива (SNF) је метод екстракције трансуранских једињења из стопљене соли, што омогућава да се добије делимично раздвајање трансуранских једињења и лантанида. Овај рад је посвећен квантно механичкој студији промена у структури, енергији и електронским особинама главне SNF компоненте, уранијум диоксида, при уклањању кисеоника из система. Такође је студиран утицај проучаваних особина на однос броја плутонијумових атома према уранијумовим атомима 1:7 и 1:3. Уклањање кисеоника доводи до сужавања јаза између трака до преласка у проводно стање при односу уранијума и кисеоника од 2:3. Јаз између трака се сужава и долази до метализације чак и када се уранијум замени са плутонијумом. Предложена је двостепена шема метализације UO_2 заснована на редукцији литијумом и директној (електронској) редукцији.

(Примљено 13. фебруара, ревидирано 22. марта, прихваћено 8. јула 2023)

REFERENCES

1. E. Curti, D.A. Kulik, *J. Nucl. Mater.* **534** (2020) 152140
(<https://doi.org/10.1016/j.jnucmat.2020.152140>)
2. D. H. Hurley, A. El-Azab, M. S. Bryan, M. W. D. Cooper, C. A. Dennett, K. Gofryk, L. He, M. Khafizov, G. H. Lander, M. E. Manley, J. M. Mann, C. A. Marianetti, K. Rickett, F. A. Selim, M. R. Tonks, J. P. Wharry, *Chem. Rev.* **122** (2022) 3711
(<https://doi.org/10.1021/acs.chemrev.1c00262>)
3. C. Ronchi, M. Sheindlin, D. Staicu, M. Kinoshita, *J. Nucl. Mater.* **327** (2004) 58
(<https://doi.org/10.1016/j.jnucmat.2004.01.018>)
4. K. Govers, S. Lemehov, M. How, M. Verwerft, *J. Nucl. Mater.* **376** (2008) 66
(<https://doi.org/10.1016/j.jnucmat.2008.01.023>)

5. S. Kihara, Z. Yoshida, H. Aoiyagi, K. Maeda , O. Shirai , Y. Kitatsuji, Y. Yoshida, *Pure Appl. Chem.* **71** (1999) 1771 (<https://doi.org/10.1351/pac199971091771>)
6. A. Y. Galashev, *Int. J. Energy Res.* **46** (2022) 3891 (<https://doi.org/10.1002/er.7458>)
7. G. L. Fredrickson, T.-S. Yoo, *J. Nucl. Mater.* **508** (2018) 51
(<https://doi.org/10.1016/j.jnucmat.2018.05.037>)
8. A.Y. Galashev, *Int. J. Energy Res.* **45** (2021) 11459 (<https://doi.org/10.1002/er.6267>)
9. T. P. Kaloni, N. Onder, J. Pencer, E. Torres, *Ann. Nucl. Energy* **144** (2020) 107511
(<https://doi.org/10.1016/j.anucene.2020.107511>)
10. J. M. Soler, E. Artacho, J. D. Gale, A. García, J. Junquera, P. Ordejón, D. Sánchez-Portal, *J. Phys.: Condens. Matter* **14** (2002) 2745 (<https://doi.org/10.1088/0953-8984/14/11/302>)
11. S. L. Dudarev, G. A. Botton, S. Y. Savrasov, C. J. Humphreys, A. P. Sutton, *Phys. Rev., B* **57** (1998) 1505 (<https://doi.org/10.1103/PhysRevB.57.1505>)
12. J. P. Perdew, A. Zunger, *Phys. Rev., B* **23** (1981) 5048
(<https://doi.org/10.1103/PhysRevB.23.5048>)
13. H. J. Monkhorst, J. D. Pack, *Phys. Rev., B* **13** (1976) 5188
(<https://doi.org/10.1103/PhysRevB.13.5188>)
14. C. L. Dugan, G. G. Peterson, A. Mock, C. Young, J. M. Mann, M. Nastasi, M. Schubert, L. Wang, W.-N. Mei, I. Tanabe, P. A. Dowben, J. Petrosky, *Eur. Phys. J., B* **91** (2018) 67
(<https://doi.org/10.1140/epjb/e2018-80489-x>)
15. H. He, D. A. Andersson, D. D. Allred, K. D. Rector, *J. Phys. Chem., C* **117** (2013) 16540
(<https://doi.org/10.1021/jp401149m>).